Design and Performance of a High-Frequency Link Induction Motor Drive Operating at Unity Power Factor

SEUNG K. SUL, MEMBER, IEEE, AND THOMAS A. LIPO, FELLOW, IEEE

Abstract—**The design and performance of a complete three-phase converter system and field-oriented induction motor drive based upon a 20-kHz ac link is described. By using the same converter for the ac input side as well as the output load side, it is shown that power can be transferred in either direction. It is also shown that, with the use of a current regulator, both power flow on the link and the link voltage amplitude can be regulated. In addition, by suitable feedback control, the power factor at the input to the converter can be adjusted to unity. Both computer and experimental results show unity power factor operation, low harmonic current in both the input and output of the system, and bidirectional power flow capability.**

INTRODUCTION

WITH RECENT advances in power electronics, variable-speed operation of an ac machine by use of frequency changers has become a well-established technology. The most widely used and highly developed frequency changers are the six-step and pulsewidth modulated (PWM) inverters which synthesize variable-frequency and variable-voltage ac output from a dc input. These inverters utilize a dc voltage link obtained by rectifying and filtering the utility source voltages.

An important factor behind the widespread use of the dc voltage link has been the ease and effectiveness by which the energy storage function, essential for decoupling the source from load, can be implemented in a dc link. Electrolytic capacitors provide low-cost high-density energy storage in the dc voltage link of a voltage source inverter. However, this type of dc-link-based power conversion system has several inherent limitations. One important drawback is the excessive switching loss and device stress that occur during switching intervals. As a result, the typical switching frequency in medium size 10–50 kW PWM inverters is, at best, 5 kHz. Because of the relatively low switching frequency, dramatic gains in important system attributes—such as faster system response, increased output frequency, improved power densities, and reduction in audible and electrical noise, particularly when the motor is operating at high speeds—are difficult to realize. Another difficulty worth mentioning is the presence of the rectifier bridge which is used to obtain dc from the ac voltage source. Conventional full-bridge rectifiers inject considerable low-order harmonics into the utility grid. In addition, the power flow is unidirectional, and regenerative operation of the system is possible only with considerable added expense.

Recently, resonant ac or dc links have been studied and suggested as strong candidates for the power conversion link. With the resonant link the switching frequency can be increased with less than proportional increases in losses or device stress by restricting switching time to the instants of zero voltage on the link [1], [2]. By increasing the resonant link frequency to 15–25 kHz, the problems associated with switching limitations can be overcome. In particular, the resonant ac link principle has recently been investigated for the power distribution system of the NASA Orbiting Space Station and as the secondary power system of advanced aircraft [3], [4] and a 20-kHz single-phase resonant voltage link has been developed for this purpose. Suitable control algorithms for an interface converter operating from a 20-kHz ac link have already been developed and verified [5], [6].

In this paper, the design and performance of a complete three-phase-to-three-phase converter system based upon a 20-kHz ac link is described. By using the same converter for the ac input side as well as the output load side, power can be readily transferred in either direction. At present, this type of topology requires 12 bidirectional switches, so that it appears to be a costly system. However, the development of new power devices such as MOS-controlled thyristor it is anticipated that cost-effective bidirectional devices will soon become available. Hence the converter described in this paper holds promise as a means for obtaining unity power factor and low harmonic current on the source side of a frequency converter as well as providing fast response with high efficiency and with no acoustic noise and markedly reduced electrical noise at the output.

OVERALL SYSTEM DESCRIPTION

The overall system described in this paper is shown in Fig. 1 wherein two converters are connected through a 20-kHz resonant link. The link voltage is supported by a parallel resonant tank circuit. Each switch of the converter has the

Paper IPCSD 89-24, approved by the Industrial Drives Committee of the IEEE Industry Applications Society for presentation at the 1988 Industry Applications Society Annual Meeting, Pittsburgh, PA, October 2-7. Manuscript released for publication July 25, 1989. This work was supported in part by the NASA Lewis Research Center, Cleveland, OH, under Contract NAG3-786.

S. K. Sul was with the Department of Electrical and Computer Engineering, University of Wisconsin, Madison, WI. He is now with the Goldstar Industrial Systems Company, Seoul, Korea.

T. A. Lipo is with the Department of Electrical and Computer Engineering, University of Wisconsin, 1415 Johnson Drive, Madison, WI 53706-1691.

IEEE Log Number 9034289.

0093-9994/90/0500-0434$01.00

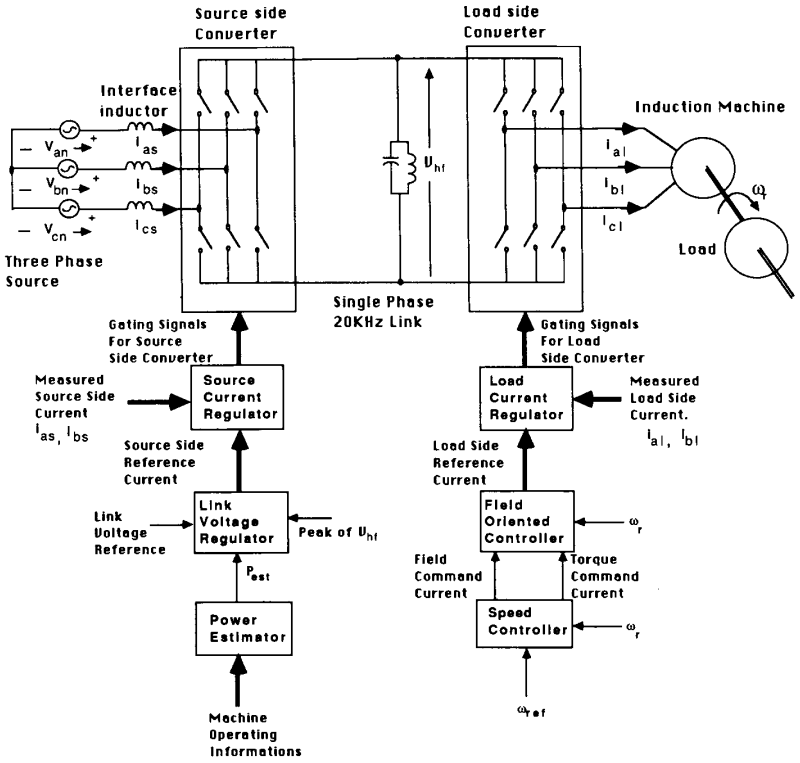

Fig. 1. Power circuit and system control block diagram.

capability of bidirectional current flow and bidirectional voltage blocking. The source side converter is nominally tied to the utility grid through interface inductors, but since these inductors are small they may not be neccessary if sufficient source impedance exists. The load side converter is connected directly to an induction machine without added capacitive filtering. The current of source side converter is controlled by a link voltage regulator which works by balancing the active power flow between the source and load. The current regulator at each converter regulates current in magnitude and phase. The power estimator provides an estimate of the current value of active power to the voltage regulator by calculating the average load power and the system losses based upon measurement of the current operating condition. The induction machine is controlled by a current-regulated field-oriented controller equipped with a speed regulation loop.

Link Voltage Regulation

For cost reasons the energy storage capacity of the link tank circuit must clearly be constructed to be smaller than the dc capacitor in a dc voltage link. To achieve a similar voltage ripple of the link would require an ac capacitor of hundreds of microfarads. Hence power balance between the load and source must be done actively. The ideal method for balancing the power flow between source and load is to measure the instantaneous power delivered to the load and system losses and deliver this exact power to the tank circuit by the source side converter. However, such an instantaneous power matching control appears impossible because of the difference in the source and load frequency and voltage.

The best approach for handling the power balancing problem is to attempt power balance only on an average basis. The instantaneous power unbalance must then be handled by a tank circuit at the cost of link voltage variations. Fortunately, a moderate variation of link voltage is not a severe problem because the power converter connected source or load has the capability of fast regulation and the current in the source and load can be controlled as desired even in the presence of high-frequency link voltage fluctuations. A small or moderate variation will, perhaps, only produce slightly more harmonic content in output current. A large variation of link voltage could, however, create more severe problems. In particular, if the voltage is instantaneously below the minimum voltage needed to synthesize the desired reference command, the actual signal will not be able to follow the reference suggesting the possibility of control instability.

Probably the most elegant approach to measuring power is by means of d, q components. That is, by

$$P=\frac{3}{2}(v_d i_d+v_q i_q).$$

In this case both the voltage and current must be measured. Since the voltage waveform has wide-band harmonics due to the modulation scheme, elimination of the harmonics requires that the cutoff frequency of the filter be set at several hundred hertz. This restriction implies several hundred microseconds of time delay. To suppress the link voltage variation within an

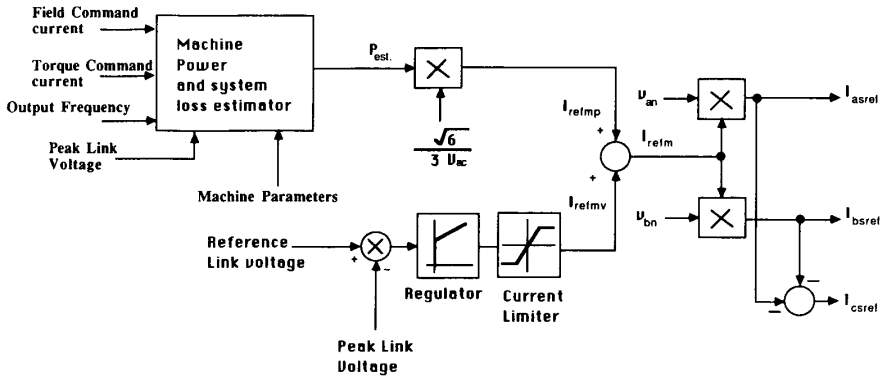

Fig. 2. Block diagram of voltage regulator. v_{ac}: source line-to-line voltage in rms. v_{an}, v_{bn}: instantaneous phase voltage of source.

acceptable level, this time delay is critical lest the capacity of the tank circuit be increased greatly.

The simplest approach for obtaining average power information is to measure the power delivered to the induction machine using a low-pass filter. However, with this method, time delays resulting from the low-pass filter are also inevitable. Thus during the delay time, the difference in average power must be covered by the power capability of the tank circuit. This observation, in turn, implies a degradation in the link voltage regulation.

Another method of obtaining average power is to estimate the power with information derived from the reference currents of the induction machine that are, in turn, available from the field-oriented controller used to control the induction machine. If the current regulation is perfect and if the machine parameters do not change and are known, the average machine power can be estimated without any time delay and without any measurement. In practice, of course, there are always differences between the actual currents and their references. Moreover, the parameters of the machine change according to flux level and operating temperature so that some error between estimated power and the actual power is inevitable. However, these errors can be compensated by using a voltage regulating loop as a minor loop. More detailed descriptions concerning the voltage control loop and power calculator can be found in [6] and [8].

A block diagram of the voltage regulator and power estimator is shown in Fig. 2 in which the source power factor is controlled as unity. The source power factor can be controlled by shifting the phase of the reference current command so long as average power balance is maintained. Hence, the input power factor can be easily programmed to be leading or lagging as desired. In the figure, the magnitude of the reference current is the sum of the value from the power estimator and the value from the link voltage regulator. The phase of the reference current is controlled according to the source voltage.

Transient Behavior of Resonant Link

A computer simulation trace illustrating link voltage buildup is shown in Fig. 3. Note that the energy from the source is pumped to the resonant tank circuit and the tank

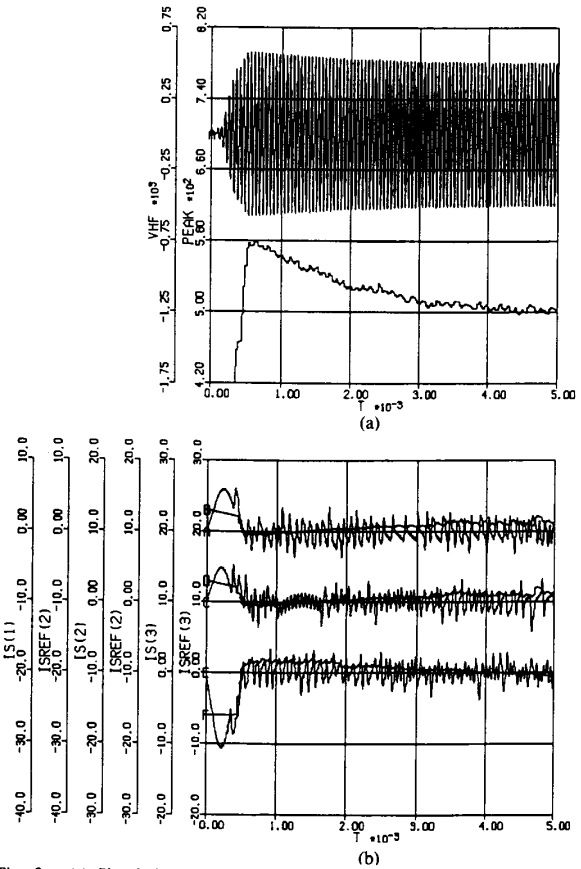

Fig. 3. (a) Simulation result of high-frequency link voltage buildup. Top trace: link voltage in volts. Bottom trace: peak amplitude of link voltage. (b) Simulation result of high-frequency link voltage buildup. From top, A is phase source current and its reference, B is phase current and its reference, and C is phase current and its reference. All traces in amperes.

voltage gradually increases to the given reference value. After overshooting, the voltage settles down to the reference value. In the simulation, the reference voltage is 500 V, and the parameters of the tank circuit are 22.5 μH, 3 μF, and 0.01 Ω. Resistance is incorporated to account for losses in the resonant tank circuit. Note that, after settling down, the source current is almost zero, supplying only the losses of the system.

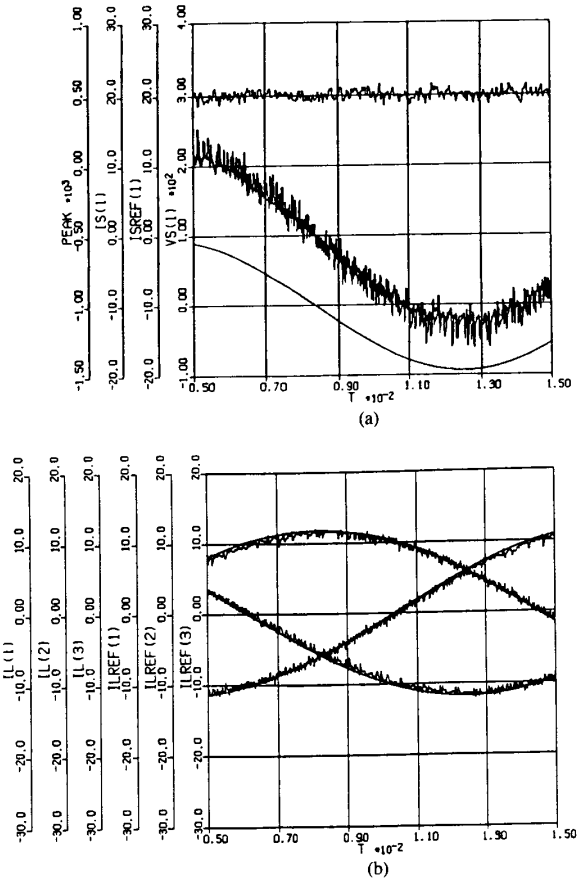

Fig. 4. (a) Simulation result of operating characteristics of system. From top: trace of peak link voltage of volts, A phase source current and its reference (A), and A phase source voltage in (V). (b) Simulation traces showing operating characteristics of system. A, B, and C phase load current and corresponding references. All traces are in amperes.

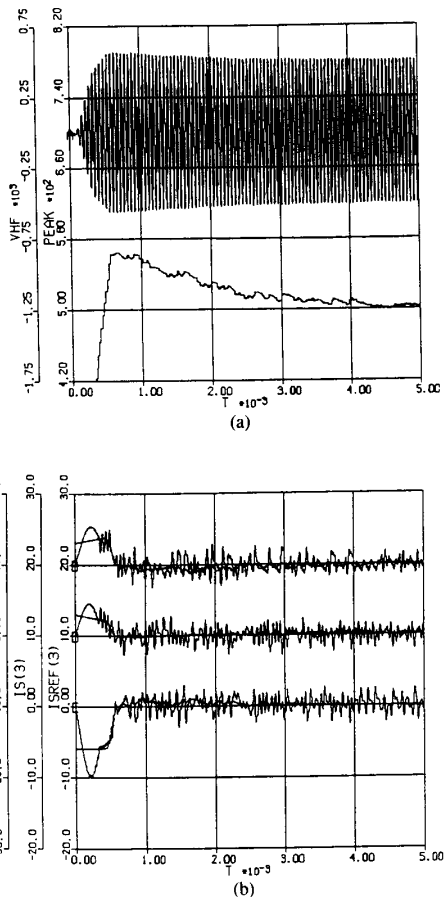

Fig. 5. (a) Simulation result of high-frequency link voltage buildup with mode controller as source current regulator. Top trace: link voltage in volts. Bottom trace: peak amplitude of link voltage. (b) Simulation result of high-frequency link voltage buildup with mode controller as source current regulator. From top: A phase source current and reference, B phase current and its reference, and C phase current and its reference. All traces in amperes.

Another simulation result illustrating the operating characteristics of the system as a whole is shown in Fig. 4. In this simulation it is assumed that a 3-hp induction machine is operating in the steady state at 40 Hz with rated torque. Observe that the link voltage amplitude is reasonably well-regulated. The A phase source current reveals unity power factor operation and indicates only very high-frequency harmonics. The synthesized load current is nearly sinusoidal and has virtually no harmonics less than 40 kHz. Clearly, the parameters of the resonant tank circuit should be traded off with the cost and performance of the system. A larger tank size can clearly provide better voltage regulation at the expense of bulkier components and increased cost.

Current Regulator

In the case of a resonant link system, the current regulators most widely used are the pulse density modulator and the delta modulator [1], [5], [7]. In general, both types of regulators are essentially identical. In the simulation the pulse density modulator was used for the current regulator. Pulse density modulation performs very well in most cases except for cases of low load inductance or when synthesizing fairly high-frequency output. Recently, the authors have reported a new type of current regulator, termed a *mode selection controller* [6], [8]. The mode selection controller operates on-line to select the switching pattern for the next switching mode that will minimize a given error function based on the predicted values of voltage and current at the next switching instant. This type of current regulator can be extended to the control of a complete bidirectional double-bridge system. Mode selection is very effective and easy to apply, especially as a source-side current regulator, where the source voltage and current can be easily measured and independent of system operating conditions. Also, by utilizing mode selection the controller can simultaneously regulate the current as well as the link voltage. In this particular case, the required error function is shown to be simply the sum of the absolute error of each phase current plus that of the link voltage.

The performance of the mode selection controller as a source current regulator is shown in Fig. 5 for the case of link voltage buildup. In these traces all parameters are identical with the case of Fig. 3 except for the current regulator. By

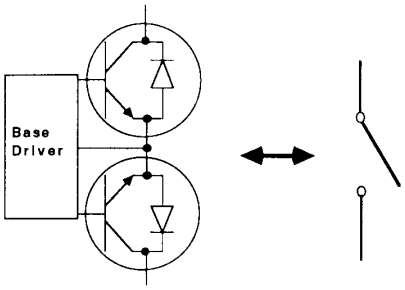

Fig. 6. Implementation of bidirectional switch.

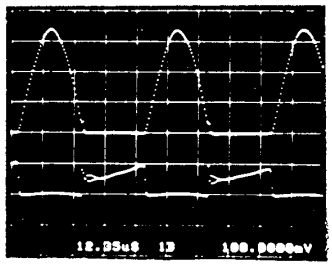

Fig. 7. Voltage and current waveform across a bidirectional switch. Top trace: voltage across switch-130 V/div; ground-4 div from bottom. Bottom trace: current across switch-5 A/div; ground-2 div from bottom. Time scale: 12.35 μs/div.

comparing Fig. 3 and Fig. 5 it can be seen that the voltage overshoot is decreased and the current ripple is also attenuated. Thus the overall performance has clearly been improved.

Experimental Results

The system shown in Fig. 1 has been constructed and thoroughly tested in the laboratory. The speed controller of Fig. 1 is the conventional proportional and integral regulator, and the indirect current regulated field orientation algorithm has been used to implement field-oriented controller. The current regulator of both the line side and load side converters employ the pulse density modulation principle. The link voltage regulator, speed controller, and power estimator were implemented by analog circuits.

The inductors used on the source side are 1.5-mH ferrite-core Litz wire inductors. In the experimental setup, two resonant tank circuits were used. The parameters of each tank are 6 μF and 11.25 μH. Two power transistors were used as a bidirectional power switch and were connected as shown in Fig. 6 [3]. Typical voltage and current wave forms across a switch during normal operation is shown in Fig. 7. As expected, the switching occurs only at the zero crossing points of the link voltage. As a load, a 3-hp 4-pole 60-Hz induction machine was employed, and the machine was mechanically coupled to a 7.5-kW dc machine to apply torque to the induction machine in the positive or negative direction.

Link Voltage Buildup

The experimental result during controlled voltage buildup is shown in Fig. 8. The trace of the peak of the link voltage reveals smooth and well-controlled behavior. Initially, the

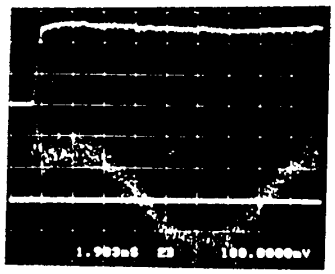

Fig. 8. Peak of high-frequency link voltage and A phase source current waveform during link voltage buildup. Top trace: peak of link voltage-130 V/div; ground-4 div from bottom. Bottom trace: A phase source current-2 A/div; ground-2 div from bottom. Time scale: 1.983 ms/div.

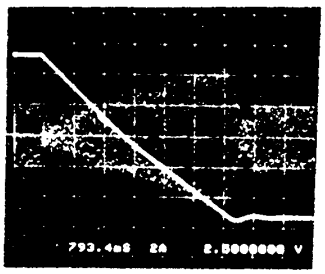

(a)

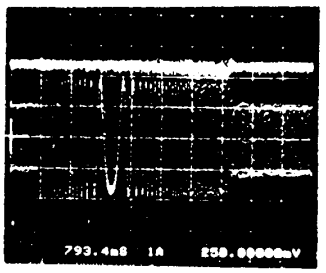

(b)

Fig. 9. (a) Response of field oriented control utilizing high-frequency link power conversion. Mechanical rotational speed-190 r/min/div; ground-4 div from bottom. A phase of source current-5 A/div; ground-4 div from bottom. Time scale: 793.4 ms/div. (b) Response of field oriented control with high-frequency link power conversion. Top trace: peak value of link voltage-130 V/div; ground-4 div from bottom. Bottom trace: induction machine A phase current-5 A/div; ground-4 div. from bottom. Time scale: 793.4 ms/div.

trace of the A phase current shows a sharp increase to store energy in the inductor. After buildup the current shows a sinusoidal variation in phase with the A phase source voltage. The difference between experimental results and simulation results is due to the difference in the loss of the modeled and actual system. In the simulation the loss component was too small compared to the real system. The real system has some losses associated with the power switch, source side inductor, and resonant tank inductor.

Dynamic Performance of Field Oriented Controller

The test results illustrating the performance of the field-oriented controller is shown in Figs. 9 and 10. In Fig. 9(a), because of large inertia of the dc machine coupled to the induction machine, it takes several seconds to accomplish the

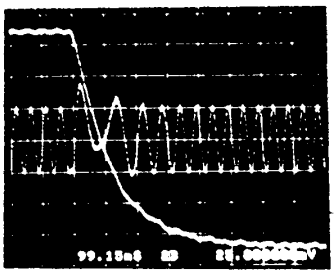

Fig. 10. Response of field-oriented control with high-frequency link power conversion without coupled dc machine. Mechanical rotational speed-190 r/min/div; ground 4 div from bottom. A phase of induction machine current-5 A/div; ground-4 div from bottom. Time scale: 99.15 ms/div.

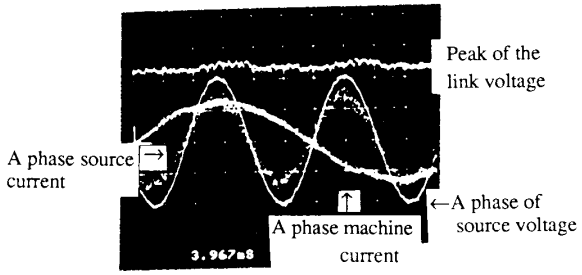

Fig. 11. Waveforms showing unity power factor operation of system during motor operation. Peak of link voltage-130 V/div. A phase of source voltage-40 V/div; A phase source current-5 A/div; A phase induction machine current-5 A/div. All grounds: 4 div from bottom. Time scale: 3.967 ms/div.

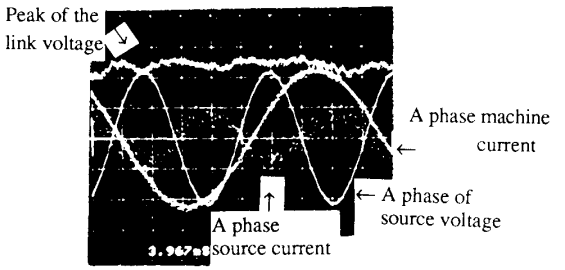

Fig. 12. System traces showing unity power factor operation of system during regeneration. Peak link voltage-130 V/div; A phase of source voltage-40 V/div; A phase of source current-5 A/div. A phase induction machine current-5 A/div. All grounds-4 div from bottom. Time scale: 3.967 ms/div.

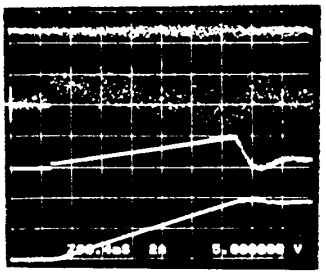

Fig. 13. Operation of power matching controller and voltage regulator. From top: peak value of link voltage-130 V/div; magnitude of reference current from voltage regulator (I_{refmv})-3.5 A/div; magnitude of reference current from power estimator (I_{refmp})-12 A/div; and mechanical rotational speed-190 r/min/div. Grounds located at 5 div, 5 div, 3 div, 0 div from bottom, respectively. Time scale: 793.4 ms/div.

speed change. While not clearly shown due to the large time scale, Fig. 9(a) shows the variation of the power of the system. Before the transient the source supplies only the loss of the system including the mechanical loss. During the deceleration time the mechanical energy is converted to electrical energy. Hence the current of the source rapidly decreases. When the machine begins to accelerate in negative direction, the current increases rapidly to supply the accelerating energy. A trace of the A phase of machine current in Fig. 9(b) clearly shows the change of the frequency as well as the phase. As shown in Fig. 9(b), the link voltage was well-regulated during speed reversal. Fig. 10 shows the system response of the same amount of speed change but this time without the coupled dc machine. The speed reversal was carried out within several tenths of a second. Both test results demonstrate the good dynamic performance of the field-oriented control incorporated with high-frequency link power conversion system.

Unity Power Factor Operation

In Figs. 11 and 12, the steady-state characteristics of the system are shown during motoring and generating operation of the induction machine. In motoring operation, shown in Fig. 11, the source supplies all the losses of the system and the mechanical energy of the induction machine. The trace of the A phase of the source current is in phase with A phase of the source voltage, which clearly demonstrates unity power factor operation. The trace of the peak of the link voltage demonstrates reasonable regulation. During generating operation shown in Fig. 12, the energy generated by the induction machine supplies all losses and the excess energy transfers to the source. Between phase A of the source voltage and the corresponding current there is 180° phase difference. The phase difference means that the source takes the energy from the system with unity power factor. The link voltage regulation for generating operation is poorer than that for motoring operation because of a slight mismatch of the parameters of the power estimator.

Power Matching Controller

As mentioned before, the high-frequency link system has no great reservoir of energy so that the power balance between source and load should be actively controlled. The behavior of the power estimation controller is shown in Fig. 13. During the starting of the induction machine the magnitude of the reference current from estimated power (I_{refmp}) was gradually increased, and after settling of the speed, the magnitude decreased to a small value to supply only the losses of the system. The reference current from voltage regulator, which is a minor loop, deviates around zero. By comparing the magnitude of the current it can be seen that a major part of the magnitude of the source reference current comes from the power estimator. The test result clearly explains the operation of the voltage regulator including the power estimator shown in Fig. 2.

Current Regulation

The characteristics of the current regulator employing pulse density modulation are shown in Figs. 14 and 15. In the case

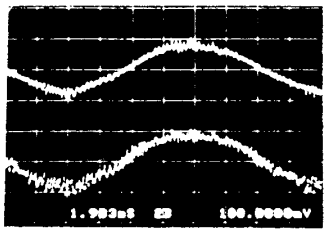

Fig. 14. System performance showing source side current regulation. Top trace: A phase source current-5 A/div; ground-5 div from bottom. Bottom trace: reference of A phase of source current-5 A/div; ground-2 div from bottom. Time scale: 1.983 ms/div.

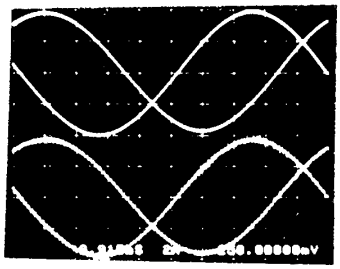

Fig. 15. Oscilloscope traces showing load side current regulation. Top trace: A and B phase induction machine current-5 A/div; ground-6 div from bottom. Bottom trace: references for A and B phase induction machine current-5 A/div; ground-2 div from bottom. Time scale: 9.915 ms/div.

of the source current regulation the reference of the source current itself has some ripples to regulate link voltage and power matching control. The actual current still accurately follows its reference. The load current reference is almost a ripple-free sinusoidal wave during steady-state operation of the induction machine. Hence the actual current shows almost the same trace with its reference. Note that during the operation of the system, no acoustic noise from the power conversion system was present because of its high switching frequency.

Conclusion

In this study a new three-phase-to-three-phase power conversion topology based upon a 20-kHz single-phase voltage link is proposed and tested by computer simulation. To demonstrate the hardware feasibility of the system and to verify the simulation results, an experimental system was built and tested. The simulation results and experimental results agree and exhibit very good load current regulation as well as unity power factor operation of the source side current. Also, the system was shown to have inherent bidirectional power flow capability. The system should prove to be a viable alternative to conventional dc link systems in the near future when bidirectional power semiconductor switches become readily available.

References

[1] P. K. Sood and T.A. Lipo, "Power conversion distribution system using a resonant high-frequency ac link," *IEEE Trans. Ind. Appl. Soc.*, Oct. 1986, pp. 533-541.

[2] D. M. Divan, "The resonant dc link converter—A new concept in static power conversion," in *Conf. Rec. Annu. Meet. IEEE Ind. Appl.*, vol. IA-24, pp. 288-300, Mar./Apr. 1988.

[3] A. C. Hoffman, I. G. Hansen, R. F. Beach *et al.*, "Advanced secondary power system for transport aircraft," NASA Tech. Paper 2463, 1985.

[4] I. G. Hansen and G. R. Sundberg, "Space station 20 khz power management and distribution system," in *Conf. Rec. 1986 Power Electronics Specialist's Conf.*, Vancouver, BC, Canada, June 1986, pp. 676-683.

[5] P. K. Sood, "High frequency link power conversion system," Ph.D. dissertation, Univ. of Wisconsin—Madison, Jan. 1987.

[6] S. K. Sul and T. A. Lipo, "Design and test of bidirectional speed and torque control of induction machines operating from high frequency link converter," NASA Rep. Contract NAG 3-786, Mar. 1988.

[7] M. Kheraluwala and D. M. Divan, "Delta modulation strategies for resonant link inverters," in *Rec. IEEE Power Electronics Specialists Conf.*, Blacksburg, VA, June 1987, pp. 271-278.

[8] S. K. Sul and T. A. Lipo, "Field oriented control of an induction machine in a high frequency link power system," presented at the IEEE Power Electronics Specialists Conf., Kyoto, Japan, Apr. 1988.

Seung K. Sul (S'78-M'87) was born in Pusan, Korea, in March 1958. He received the B.S., M.S., and Ph.D. degrees from Seoul National University, Seoul, Korea, in 1980, 1983, and 1986, respectively.

He was a Visiting Research Associate at the University of Wisconsin—Madison from 1986 to 1988. He is now with Goldstar Industrial Systems Company, in Seoul, Korea, as a Principal Research Engineer. His current research interests are in high-frequency resonant inverter for high power applications and digital signal processing of machine drive systems.

Thomas A. Lipo (M'64-SM'71-F'87), for a photograph and biography please see page 433 of this issue.